Journal of Applied Analysis and Computation
Volume 9, Number 2, April 2019, 810–828
Website:http://jaac.ijournal.cn
DOI:10.11948/2156-907X.20190028

# SOLITARY WAVES, PERIODIC PEAKONS, PSEUDO-PEAKONS AND COMPACTONS GIVEN BY THREE ION-ACOUSTIC WAVE MODELS IN ELECTRON PLASMAS

Yan Zhou[1,2†], Jie Song[1] and Tong Han[3]

**Abstract** The nonlinear ion-acoustic oscillations models are governed by three partial differential equation systems. Their travelling wave equations are three first class singular traveling wave systems depending on different parameter groups, respectively. By using the method of dynamical system and the theory of singular traveling wave systems, in this paper, it is shown that there exist parameter groups such that these singular systems have solitary wave solutions, pseudo-peakons, periodic peakons and compactons as well as kink and anti-kink wave solutions. The results of this paper complete the studies of three papers [5, 13] and [14].

**Keywords** Bifurcation, singular travelling wave system, solitary wave solution, pseudo-peakon, periodic peakon, compacton, kink and anti-kink wave.

**MSC(2010)** 34C60, 35Q51, 35C05, 35C07, 35C08.

## 1. Introduction

Recently, in 2018 and 2019, three dynamical models are considered by three papers (Rufai and Bharuthram [13], Hatami and Tribeche [5], Sultana and Schlickeiser [14]), respectively. The authors applied so called Sagdeev potentials to investigate solitary wave solutions given by these models. However they did not study the dynamical systems corresponding to the Sagdeev potentials, and did not know the existence of singular straight lines in the differential systems describing the traveling waves. In addition, they did not understand the theory of singular traveling wave system developed by Li and Chen [7] and Li [8]. Therefore, these three papers can not discuss existence of the pseudo-peakons, periodic peakons, compactons as well as kink and anti-kink wave solutions. Similar cases appeared in Ghebache and Tribeche [2, 3] and Das [1]. The three papers [10–12] have obtained some new complete results by using the method of dynamical system. It is necessary to

†The corresponding author. Email address:zy4233@hqu.edu.cn(Y. Zhou)
[1]School of Mathematical Sciences, Huaqiao University, Quanzhou, Fujian 362021, China
[2]Wu Wen-Tsun Key Laboratory, School of Mathematical Sciences, University of Science and Technology of China, Hefei, Anhui 230026, China
[3]Shengxiang School of Business, Shanghai Sanda University, Shanghai, 201209, China
*This research was partially supported by the National Natural Science Foundation of China (11871231,11162020).

study the dynamical behaviors of the traveling wave solutions of the following three models.

**1.** Hatami and Tribeche [5] stated that "One of the most important longitudinal electrostatic waves in plasma is the ion-acoustic wave that can be observed commonly in space and laboratory plasmas. According to theoretical as well as experimental results, this wave plays an important role in the turbulence heating, the laser plasma interaction, the particle acceleration, etc." Considering a homogeneous, collisionless, unmagnetized plasma consisting of ion with finite temperature and two species of $q$-nonextensive electrons (cool and hot), the normalized basic equations, based on the fluid description, for one dimensional propagation of nonlinear ion-acoustic solitary waves in such a plasma are given as follows:

$$\begin{aligned}
&\tfrac{\partial N_i}{\partial \tau} + \tfrac{\partial (N_i u_i)}{\partial X} = 0,\\
&\tfrac{\partial u_i}{\partial \tau} + u_i \tfrac{\partial u_i}{\partial X} + \tfrac{\sigma}{N_i}\tfrac{\partial P_i}{\partial X} = -\tfrac{\partial \phi}{\partial X},\\
&\tfrac{\partial P_i}{\partial \tau} + u_i \tfrac{\partial P_i}{\partial X} + 3P_i \tfrac{\partial u_i}{\partial X} = 0,\\
&\tfrac{\partial^2 \phi}{\partial X^2} = \delta N_c + (1-\delta)N_h - N_i,
\end{aligned} \tag{1.1}$$

where $N_{j=i,c,h} = \frac{n_j}{n_{j0}}, u_i = \frac{v_i}{C_s}, C_s = \sqrt{\frac{T_c}{m_i}}, \sigma = \frac{T_i}{T_c}, \phi = \frac{e\varphi}{T_c}, \delta = \frac{N_{c0}}{N_{i0}}, \tau = t\omega_{pi}, \omega_{pi} = \sqrt{\frac{4\pi e^2 n_{i0}}{m_i}}, X = \frac{x}{\lambda_D}, \lambda_D = \sqrt{\frac{T_c}{4e^2\pi n_{i0}}}$ and $\beta = \frac{T_c}{T_h}$. The normalized densities of the q-distributed electrons are given by

$$N_c = [1 + (q_c - 1)\phi]^{\frac{(q_c+1))}{2(q_c-1)}}, \quad N_h = [1 + \beta(q_h - 1)\phi]^{\frac{(q_h+1))}{2(q_h-1)}}. \tag{1.2}$$

In order to derive the Sagdeev's pseudo potential from system (1.1), we assume that all the variables depend on a single independent variable $\xi = X - V\tau$, where $V$ is the velocity of the moving frame. Further, the following appropriate boundary conditions $\phi \to 0, u_i \to u_{i0}, N_i \to 1, P_i \to 1$ at $|\xi| \to \infty$ are defined. Thus, system (1.1) can be reduced. Especially, the forth equation of system (1.1) becomes

$$\frac{d^2\phi}{d\xi^2} = \delta N_c + (1-\delta)N_h, -N_i, \tag{1.3}$$

where

$$N_i = \frac{1}{2\sqrt{3\sigma}}\left\{\sqrt{(M+\sqrt{3\sigma})^2 - 2\phi} - \sqrt{(M-\sqrt{3\sigma})^2 - 2\phi}\right\}, \ M = V - u_{i0}$$

is the Mach number.

Then, Hatami and Tribeche [5] obtained the following two-order differential equation:

$$\begin{aligned}
\tfrac{d^2\phi}{d\xi^2} &= \delta[1 + (q_c - 1)\phi]^{\frac{(q_c+1))}{2(q_c-1)}} + (1-\delta)[1 + \beta(q_h - 1)\phi]^{\frac{(q_h+1))}{2(q_h-1)}}\\
&\quad - \tfrac{1}{2\sqrt{3\sigma}}\left\{\sqrt{(M+\sqrt{3\sigma})^2 - 2\phi} - \sqrt{(M-\sqrt{3\sigma})^2 - 2\phi}\right\}.
\end{aligned} \tag{1.4}$$

It is equivalent to the planar dynamical system

$$\begin{aligned}\frac{d\phi}{d\xi} &= y,\\ \frac{dy}{d\xi} &= \delta[1+(q_c-1)\phi]^{\frac{(q_c+1))}{2(q_c-1)}} + (1-\delta)[1+\beta(q_h-1)\phi]^{\frac{(q_h+1))}{2(q_h-1)}}\\ &\quad -\frac{1}{2\sqrt{3\sigma}}\left\{\sqrt{(M+\sqrt{3\sigma})^2-2\phi}-\sqrt{(M-\sqrt{3\sigma})^2-2\phi}\right\}\equiv Q_1(\phi),\end{aligned} \tag{1.5}$$

which has the first integral or Hamiltonian:

$$H_1(\phi,y)=\frac{1}{2}y^2+S_1(\phi)=h, \tag{1.6}$$

where

$$\begin{aligned}S_1(\phi)&=\frac{2\delta}{3q_c-1}\left\{1-[1+(q_c-1)\phi]^{\frac{3q_c-1}{2(q_c-1)}}\right\}+\frac{2(1-\delta}{\beta(3q_h-1)}\left\{1-[1+\beta(q_h-1)\phi]^{\frac{3q_h-1}{2(q_h-1)}}\right\}\\ &-\frac{1}{6\sqrt{3\sigma}}\left\{\left[(M+\sqrt{3\sigma})^2-2\phi\right]^{\frac{3}{2}}-(M+\sqrt{3\sigma})^3-\left[(M-\sqrt{3\sigma})^2-2\phi\right]^{\frac{3}{2}}+(M-\sqrt{3\sigma})^3\right\}\end{aligned} \tag{1.7}$$

is called Sagdeev's pseudo potential. We notice that [5] did not study the dynamics of system (1.5). By using the numerical method, the authors only considered the Sagdeev potential (see Sagdeev [15]).

**2.** Sultana and Schlickeiser [14] considered fully nonlinear heavy ion-acoustic solitary waves in astrophysical degenerate relativistic quantum plasmas. The heavy ion-acoustic wave, in which the inertia (the restoring force) is provided by the mass density of the heavy ion species (the degenerate pressures of the electron and light ion species), is described by the following one dimensional normalized equations:

$$\begin{aligned}&\frac{\partial n_h}{\partial t}+\frac{\partial(n_h u_h)}{\partial x}=0,\\ &\frac{\partial u_h}{\partial t}+u_h\frac{\partial u_h}{\partial x}=-\frac{\partial\phi}{\partial x},\\ &K_1\frac{\partial {n_i}^{\gamma_i}}{\partial x}+n_i\frac{\partial\phi}{\partial x}=0,\\ &K_2\frac{\partial {n_e}^{\gamma_e}}{\partial x}-n_e\frac{\partial\phi}{\partial x}=0,\\ &\frac{\partial^2\phi}{\partial x^2}=(1+\alpha)n_e-\alpha n_i-n_h,\end{aligned} \tag{1.8}$$

where the number density $n_s$ is normalized by its equilibrium value $n_{s0}$, heavy ion fluid velocity $u_h$ is normalized by the heavy ion sound speed $c_0=(z_h m_e c^2/m_h)^{1/2}$, the electrostatic potential $\phi$ is normalized by $m_e c^2/e$. The space $x$ and time $t$ are normalized by the Debye length $\lambda_0=(m_e c^2/4\pi e^2 z_h n_{h0})^{\frac{1}{2}}$ and the plasma period $\omega_{ph}^{-1}=(4\phi z_h^2 e^2 n_{h0}/m_h)^{-\frac{1}{2}}$ of the heavy ion species, respectively. Other parameters are defined as $\alpha=z_i n_{i0}/z_h n_{h0}, K_1=K_i {n_{i0}}^{\gamma_i-1}/z_i m_e c^2$ and $K_2=K_e {n_{e0}}^{\gamma_e-1}/m_e c^2$.

By integrating the third and fourth equations over $x$, we obtain the number densities (normalized) of the inertialess degenerate light ion $n_i$ and electron $n_e$:

$$n_i=\left(1-\frac{\gamma_i-1}{\gamma_i K_1}\phi\right)^{\frac{1}{\gamma_i-1}},\quad n_e=\left(1+\frac{\gamma_e-1}{\gamma_e K_2}\phi\right)^{\frac{1}{\gamma_e-1}}, \tag{1.9}$$

where $\gamma_i(\gamma_e)$ represents the relativistic index of the light ion (electron) species, and $\gamma_i = \frac{5}{3}$ will be considered for the non-relativistically degenerate light ion species for our analysis purposes. Now, substituting (1.9) into the fifth equation, we obtain

$$\frac{\partial^2\phi}{\partial x^2} = (1+\alpha)\left(1+\frac{\gamma_e-1}{\gamma_e K_2}\phi\right)^{\frac{1}{\gamma_e-1}} - \alpha\left(1-\frac{\gamma_i-1}{\gamma_i K_1}\phi\right)^{\frac{1}{\gamma_i-1}} - n_h. \tag{1.10}$$

Assume that $\phi$ depends on a single travelling variable $\xi = x - Mt$ (where $M$ is Mach number, normalized by the heavy ion sound speed $c_0$). By applying the steady state condition, and imposing the appropriate boundary conditions (namely, $n_h \to 1, u_h \to 0, \phi \to 0$, and $\frac{d\phi}{d\xi} \to 0$ at $\xi \to \pm\infty$), the plasma model equations (1.8) are reduced to the energy integral(see [14]):

$$\frac{1}{2}\left(\frac{d\phi}{d\xi}\right)^2 + \Psi(\phi) = 0, \tag{1.11}$$

where the (Sagdeev-type) pseudo-potential (see [15]) is given by

$$\begin{aligned}\Psi(\phi) = M^2\left[1-\left(1-\tfrac{2\phi}{M^2}\right)^{\frac{1}{2}}\right] + \alpha K_1\left[1-\left(1-\tfrac{\gamma_i-1}{\gamma_i K_1}\phi\right)^{\frac{1}{\gamma_i-1}}\right]\\ +(1+\alpha)K_2\left[1-\left(1+\tfrac{\gamma_e-1}{\gamma_e K_2}\phi\right)^{\frac{1}{\gamma_e-1}}\right].\end{aligned} \tag{1.12}$$

Clearly, corresponding to the Hamiltonian function $H_2(\phi, y) = \frac{1}{2}y^2 + \Psi(\phi) = h$, we have the dynamical system:

$$\frac{d\phi}{d\xi} = y, \frac{dy}{d\xi} = -\frac{1}{\sqrt{1-\frac{2\phi}{M^2}}} - \alpha\left(1-\frac{\phi}{\beta_1 K_1}\right)^{\beta_1-1} + (1+\alpha)\left(1+\frac{\phi}{\beta_2 K_2}\right)^{\beta_2-1} \equiv Q_2(\phi), \tag{1.13}$$

where $\beta_1 = \frac{\gamma_i}{\gamma_i-1}, \beta_2 = \frac{\gamma_e}{\gamma_e-1}$.

Sultana and Schlickeiser [14] did not derived system (1.13) and did not study its dynamics. By using the numerical method, the authors only considered the Sagdeev potential (1.11).

**3.** In [13], Rufai and Bharuthram considered a homogeneous, magnetized three-component, collisionless plasma consisting of electrons $(N_e, T_e)$, protons $(N_p, T_p)$ and a cold singly-charged oxygen-ion beam $(N_i, T_i = 0)$ drifting along the magnetic field direction $\mathbf{B}_0 = B_0\hat{z}$ with speed $v_0$ , where $N_j(T_j)$ is the density (temperature) of the $j-$th species. Satellite observations have recorded the existence of such a beam. Waves propagate in $(x, z)$-plane at an angle which changes from $\theta_0$ to $\mathbf{B}_0$. Then, the normalized fluid governing equations are given by:

$$\begin{aligned}&\tfrac{\partial n_i}{\partial t} + \tfrac{\partial(n_i v_x)}{\partial x} + \tfrac{\partial(n_i v_z)}{\partial z} = 0,\\ &\tfrac{\partial v_x}{\partial t} + (v_x\tfrac{\partial}{\partial x} + v_z\tfrac{\partial}{\partial z})v_x = -\tfrac{\partial\psi}{\partial x} + v_y,\\ &\tfrac{\partial v_y}{\partial t} + (v_x\tfrac{\partial}{\partial x} + v_z\tfrac{\partial}{\partial z})v_y = -v_x,\\ &\tfrac{\partial v_z}{\partial t} + (v_x\tfrac{\partial}{\partial x} + v_z\tfrac{\partial}{\partial z})v_z = -\tfrac{\partial\psi}{\partial z},\end{aligned} \tag{1.14}$$

where $n_i$ is the oxygen ion density, $v_x, v_y$ and $v_z$ are the components of the oxygen ion velocity along $x, y$, and $z$ directions respectively, $\psi$ is the waves electrostatic potential. We may use the Boltzmann distribution for the thermal electrons $n_e = \exp(\psi)$ and protons $n_p = (1-p)\exp(-\alpha_p\psi)$. In the above equations, the charge neutrality condition at equilibrium is given by $N_{e0} = N_{i0} + N_{p0}$. The uses of normalization are following: densities are normalized by the electron density $N_{e0}$ , velocities are normalized by the speed $C_s = (T_e/m_i)^{\frac{1}{2}}$ (where $m_i$ is the oxygen ion mass), distance is normalized by the ion Larmor radius $\rho_i = \frac{C_s}{\Omega}$, time $t$ is normalized by the inverse of oxygen-ion gyro-frequency $\Omega^{-1}(\Omega = \frac{eB_0}{m_i c})$, and electrostatic potential $\phi$ is normalized by $\frac{T_e}{e}$ , where $\psi = \frac{e\phi}{T_e}$. Then, we have $p = \frac{N_{i0}}{N_{e0}}$ and the temperature ratio $\alpha_p = \frac{T_e}{T_p}$. This system is closed with the quasi-neutrality condition which is valid for low-frequency phenomena, i.e. $n_i + n_p = n_e$. We have

$$n_i(\psi) = \exp(\psi) - (1-p)\exp(-\alpha_p\psi), \quad n_i'(\psi) = \exp(\psi) + (1-p)\alpha_p\exp(-\alpha_p\psi). \tag{1.15}$$

By a localized stationary frame $\xi = \frac{1}{M}(\alpha x + \gamma z - Mt)$, where $M = \frac{V}{c_s}$ is the Mach number, under some appropriate boundary conditions for localized solutions, for example $v_z = v_0$, Rufai and Bharuthram [13] obtain the following "energy integral" of an oscillating particle of unit mass with pseudo-potential $S_3(\psi)$:

$$\frac{1}{2}\left(\frac{d\psi}{d\xi}\right)^2 + S_3(\psi) = 0, \tag{1.16}$$

where

$$S_3(\psi) = -\left[\frac{A(\psi) + B(\psi)}{C(\psi)}\right], \tag{1.17}$$

$$A(\psi) = -\frac{M^2M_d^2(n_i(\psi)-p)^2}{2n_i^2(\psi)} - M^2(1-\gamma^2)\psi, \quad C(\psi) = \left(1 - \frac{M_d^2p^2n_i'(\psi)}{n_i^3(\psi)}\right)^2, \tag{1.18}$$

$$B(\psi) = \frac{M^2H_0(\psi)}{p}\left(1 - \frac{p\gamma^2}{n_i(\psi)} - \frac{\gamma^2H_0(\psi)}{2M_d^2p}\right), \quad M_d = M - \gamma v_0 \tag{1.19}$$

and

$$H_0(\psi) = \exp(\psi) - 1 + \frac{1-p}{\alpha_p}(\exp(-\alpha_p\psi) - 1). \tag{1.20}$$

By examining the pseudo potential $S_3(\psi)$, [13] analyzed the conditions under which the energy integral (1.16) leads to a solitary wave solution. The author did not consider the following dynamical system:

$$\begin{aligned} \tfrac{d\psi}{d\xi} &= y, \\ \tfrac{dy}{d\xi} &= -S_3'(\psi) = Q_3(\psi) = \tfrac{n_i^6(\psi)[(A(\psi)+B(\psi))C'(\psi) - C(\psi)(A'(\psi)+B'(\psi))]}{(n_i^3(\psi) - p^2M_d^2n_i'(\psi))^4}. \end{aligned} \tag{1.21}$$

The system (1.21) has Hamiltonian function

$$\frac{1}{2}y^2 + S_3(\psi) = h. \tag{1.22}$$

We can write that

$$\begin{aligned} S_3(\psi) = \tfrac{M^2(n_i(\psi))^4}{(D(\psi))^4}\Big[&-\tfrac{1}{2}M_d^2(n_i(\psi)-p)^2 - (1-\gamma^2)\psi(n_i(\psi))^2 + \tfrac{1}{p}(n_i(\psi))^2H_0(\psi) \\ &-\tfrac{\gamma^2}{2M_d^2p^2}(H_0(\psi))^2(n_i(\psi))^2 - \gamma^2H_0(\psi)n_i(\psi)\Big], \end{aligned} \tag{1.23}$$

where $D(\psi) = n_i^3(\psi) - p^2 M_d^2 n_i'(\psi)$.

In order to finish the studies about the traveling wave solutions of system (1.1), (1.8) and (1.14), in this paper, we use the method of dynamical system to discuss the dynamical behaviors of systems (1.5), (1.13) and (1.21). We notice that

(i) When $0 < q_c < 1, 0 < q_h < 1$, system (1.5) is the first class singular nonlinear traveling wave system defined in [7] and [8], which has two singular straight lines $\phi = \phi_{sc} = \frac{1}{1-q_c}$ and $\phi = \phi_{sh} = \frac{1}{\beta(1-q_h)}$.

(ii) When $\gamma_i > 1$ and $\gamma_e > 1$, system (1.13) is the first class singular nonlinear traveling wave system with the singular straight line $\phi = \frac{1}{2}M^2$.

(iii) When $0 < p < 1$, if the function $D(\psi)$ has a unique zero $\psi = \psi_s$, then system (1.21) is the first class singular nonlinear traveling wave system with the singular straight line $\psi = \psi_s$.

It is very interesting that singular traveling systems have peakon, pseudo-peakon, periodic peakon and compacton family. Periodic peakon is a classical solution with two time scales of a singular traveling system. Peakon is a limit solution of a family of periodic peakons, or a limit solution of a family of pseudo-peakons under two classes of limit senses (see Li, J., et al. [9]). Compacton family is a solution family for which all solutions $\phi(\xi)$ have finite support set, i.e., the defined region of every $\phi(\xi)$ with respect to $\xi$ is finite and the value region of $\phi$ is bounded. Corresponding to different types of phase orbits, the authors gave a classification for different wave profiles of $\phi(\xi)$ in [6,7] and [8].

The theory of the singular traveling wave system developed by [7] and [8] is very useful. We will use this theory to analyze the wave profiles of the solution functions $\phi(\xi)$ and $\psi(\xi)$ of systems (1.5), (1.13) and (1.21). We know the following relationships between a wave profile of $\phi(\xi)$ or $\psi(\xi)$ and a phase orbit of these planar dynamical systems.

(1) A smooth homoclinic orbit to a saddle point of a traveling wave system gives rise to a smooth solitary wave solution of a PDE.

(2) A smooth heteroclinic loop connecting two saddle points of a traveling wave system gives rise to a kink wave solution or an anti-kink wave solution of a PDE.

(3) For a homoclinic orbit, if it has a segment that completely lies in a left (or right) small strip neighborhood of a singular straight line, then this homoclinic orbit defines a pseudo-peakon solution of system.

(4) If there exists a curve triangle connecting saddle points and surrounding the periodic annulus of a center of a traveling wave system, in the neighborhood of a singular straight line (for which a segment is an edge of the triangle), then as a limit curve of a family of periodic orbits, this curve triangle gives rise to a peakon solution of system.

(5) For a family of periodic orbits, if each orbit of the family has a segment which completely lies in a left (or right) small strip neighborhood of a singular straight line, then these periodic orbits determine a family of periodic peakon solutions of system.

(6) For a family of open orbits, when $|y| \to \infty$, if these orbits tend to a singular straight line, then this open orbit family gives rise to a family of compactons.

(7) For a family of periodic orbits, if each periodic orbit of the family transversely intersects a singular straight line, then this periodic orbit family gives rise to a family of compactons.

With respect to the existence of solitary wave solutions, we have the following

conclusion which is a theoretical and general result depending on the three parameter groups of three systems.

**Theorem 1.1.** *(i) The origin $O(0,0)$ of system (1.5) is a saddle point if and only if*

$$M > \sqrt{3\sigma + \frac{2}{\delta(1+q_c)+(1-\delta)\beta(1+q_h)}}.$$

*Under this condition, if there exists a homoclinoc orbit of system (1.5) to the origin $O(0,0)$, then it gives rise to a solitary wave solution or a pseudo-peakon solution of system (1.1).*

*(ii) The origin $O(0,0)$ of system (1.13) is a saddle point if and only if*

$$M > \frac{1}{\sqrt{\frac{\alpha}{K_1}\left(1-\frac{1}{\beta_1}\right)+\frac{1+\alpha}{K_2}\left(1-\frac{1}{\beta_2}\right)}}.$$

*Under this condition, if there exists a homoclinoc orbit of system (1.13) to the origin $O(0,0)$, then it gives rise to a solitary wave solution or a pseudo-peakon solution of system (1.8).*

*(iii) Assume that $0 < p < 1$. The origin $O(0,0)$ of system (1.21) is a saddle point if and only if*

$$M_{cusp} \equiv \gamma\left(v_0 + \sqrt{\frac{p}{1+\alpha_p(1-p)}}\right) < M < \left(\gamma v_0 + \sqrt{\frac{p}{1+\alpha_p(1-p)}}\right) \equiv M_{inf}.$$

*Under this condition, if there exists a homoclinoc orbit of system (1.21) to the origin $O(0,0)$, then it gives rise to a smooth solitary wave solution of system (1.14).*

The proof of this theorem is showed in the following section 2, 3 and 4.

This paper is organized as follows. In section 2, 3 and 4, we investigate the bifurcations of phase portraits of system (1.5), (1.13) and (1.21), and discuss the existence of solitary wave solutions, pseudo-peakons, periodic peakons and compactons as well as kink and anti-kink wave solutions of these systems.

## 2. Bifurcations of phase portraits and dynamical behaviors of solutions of traveling wave system (1.5)

In this section, we consider possible bifurcations of phase portraits of system (1.5). To investigate the equilibrium points $E_j(\phi_j, 0)$ of system (1.5), we need to discuss the zeros $\phi_j$ of the function $Q_1(\phi)$. Clearly, $Q_1(0) = 0$, thus the origin $O(0,0)$ is an equilibrium point of system (1.5). Because $Q_1(\phi)$ depends on the six-parameter group $(\beta, \delta, \sigma, q_c, q_h, M)$, so it is very difficult to find other equilibrium points of system (1.5) depending on the changes of parameters. We assume that the parameters $q_c$ and $q_h$ are rational numbers and $\frac{1}{3} < q_c < 1, \frac{1}{3} < q_h < 1$. In this case, the exponents $\beta_c = \frac{q_c+1}{2(q_c-1)}, \beta_h = \frac{q_h+1}{2(q_h-1)}$ are negative number. Function $Q_1(\phi)$ is defined in the interval $(-\infty, \phi_d)$, where $\phi_d = \min(\phi_{sc}, \phi_{sh}, \phi_m), \phi_m = \frac{1}{2}(M - \sqrt{3\sigma})$. For a given parameter group, we can use numerical method to find the zeros of $Q_1(\phi)$ in $(-\infty, \phi_d)$.

Let $M(\phi_j,0)$ be the coefficient matrix of the linearized system of system (1.5) at an equilibrium point $E_j(\phi_j,0)$ and $J(\phi_j,0)=\det M(\phi_j,0)$. We have $J(\phi_j,0)=-Q_1'(\phi_j)$, when $M>\sqrt{3\sigma}$,

$$J(0,0)=-\frac{1}{2}\delta(1+q_c)-\frac{1}{2}(1-\delta)\beta(1+q_h)+\frac{1}{M^2-3\sigma}.$$

By the theory of planar dynamical system (see [8]), for an equilibrium point of a planar Hamiltonian system, if $J<0$ $(>0)$, then the equilibrium point is a saddle point (a center point); if $J=0$ and the Poincaré index of the equilibrium point is 0, then this equilibrium point is a cusp. When $M=\sqrt{3\sigma+\frac{2}{\delta(1+q_c)+(1-\delta)\beta(1+q_h)}}\equiv M_b$, or $\beta=\frac{2-(M^2-3\sigma)(1+q_c)\delta)}{(M^2-3\sigma)(1-\delta)(1+q_h)}\equiv\beta_b$, we get $J(0,0)=0$, so that the origin $O(0,0)$ is a cusp. When $M>M_b$ $(M<M_b)$, the origin is a saddle point (a center).

Write that $h_j=H_1(\phi_j,0)$, where $(\phi_j,0)$ is an equilibrium point of system (1.5) with $-\infty<\phi<\phi_d, h_0=H(0,0)=0$.

For the fixed parameter values: $\beta=0.1,\delta=0.25,q_c=0.5,q_h=0.75,\sigma=0.2$, by varying the parameter $M$, we can obtain the different graphs of function $Q_1(\phi)$. Some graphs are shown in Fig.1 (a)-(d). In these cases, system (1.5) has 4 equilibrium points. From these graphs we know that when $\phi\to\phi_m$, $Q_1(\phi)\to-\infty$.

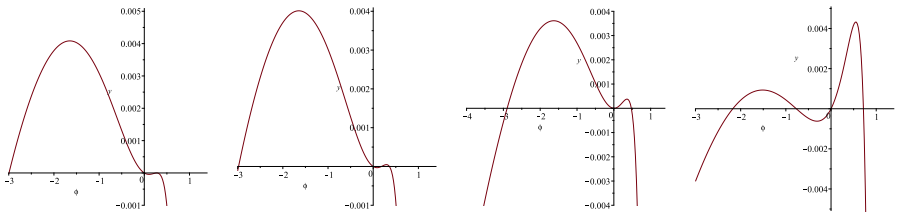

(a) $M=2.130053$ (b) $M=2.1305$ (c) $M=M_b$ (d) $M=2.15$

**Figure 1.** The graphs of function $Q_1(\phi)$ as $M$ is varied. Parameter values: $\beta=0.1,\delta=0.25,q_c=0.5,q_h=0.75,\sigma=0.2;M_b=2.133217589$.

Using the above results, we have the following bifurcations of phase portraits of traveling wave system (1.5):

For the fixed parameter values: $\delta=0.18,q_c=0.16,q_h=0.75,M=2.15,\sigma=0.12$, by changing the parameter $\beta$, we have the following bifurcations of phase portraits of traveling wave system (1.5):

We see from Fig.2 (c)-(j) that in the left strip neighborhood of the straight line $\phi=\phi_m$, there exists a family of segments of the periodic orbits of system (1.5), which is very close to the straight line $\phi=\phi_m$. Along these segments of periodic orbits, the motions of phase points are fast. In fact, by using the first equation, for a periodic orbit in the left strip neighborhood of the straight line $\phi=\phi_m$, we obtain its period

$$T=\oint\frac{d\phi}{y(\phi)}=\int_{\phi_0}^{\phi_+}\frac{d\phi}{y(\phi)}+\int_{\phi_-}^{\phi_0}\frac{d\phi}{y(\phi)}+\int_{\phi_+}^{\phi_-}\frac{d\phi}{y(\phi)}=T_1+T_2+O(\epsilon),\qquad(2.1)$$

where $(\phi_0,0)$ is the left intersection point of the periodic orbit and the $\phi-$axis, $(\phi_+,y_+)$ and $(\phi_+,y_-)$ are the upper point and lower point of the segment of the

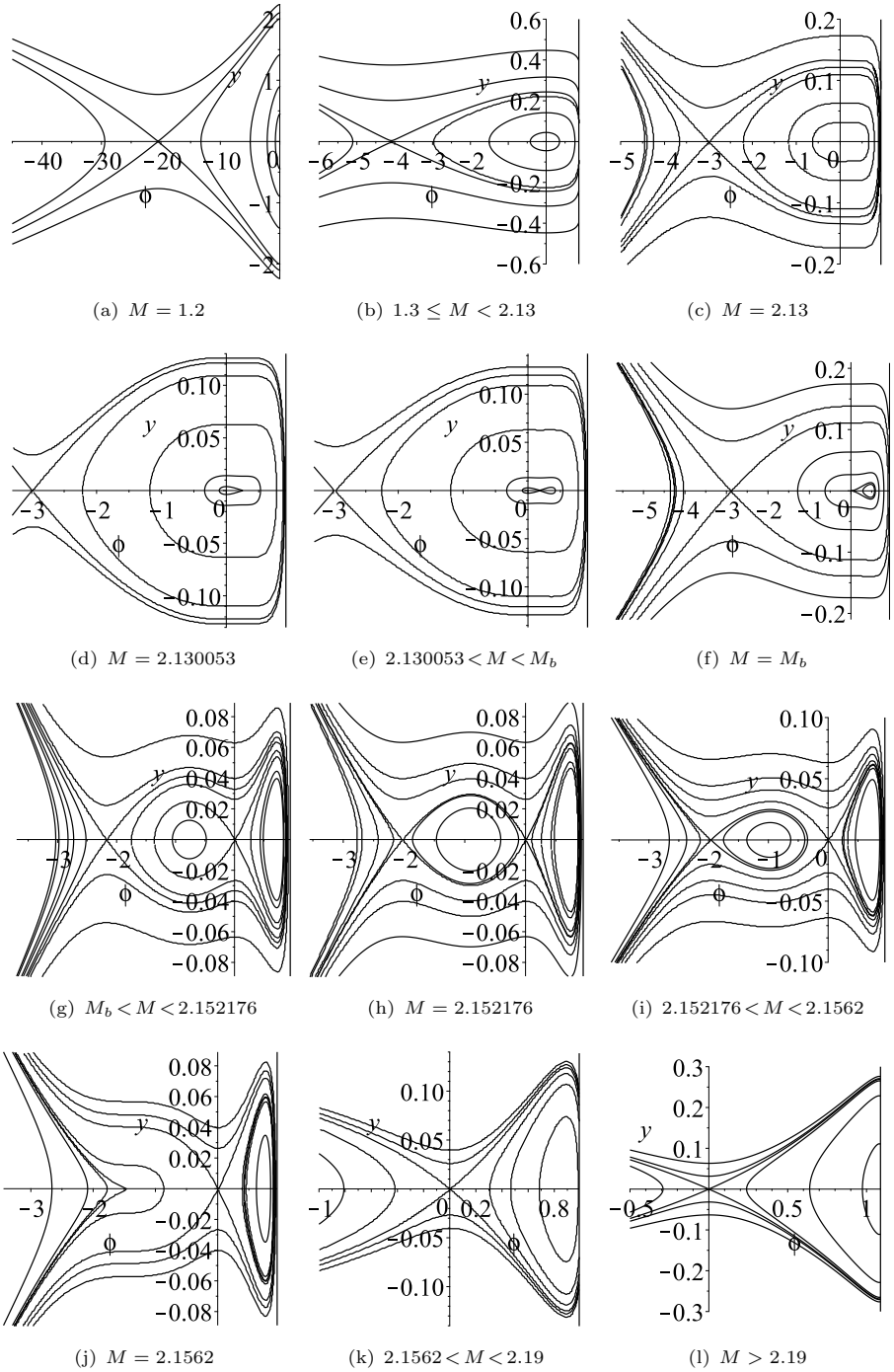


(a) $M = 1.2$ (b) $1.3 \le M < 2.13$ (c) $M = 2.13$

(d) $M = 2.130053$ (e) $2.130053 < M < M_b$ (f) $M = M_b$

(g) $M_b < M < 2.152176$ (h) $M = 2.152176$ (i) $2.152176 < M < 2.1562$

(j) $M = 2.1562$ (k) $2.1562 < M < 2.19$ (l) $M > 2.19$

**Figure 2.** The bifurcations of phase portraits of system (1.5) as $M$ is varied. Parameter values: $\beta = 0.1, \delta = 0.25, q_c = 0.5, q_h = 0.75, \sigma = 0.2$; $M_b = 2.133217589$.

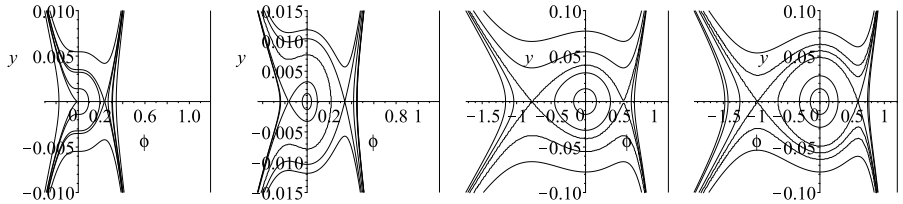


(a) $\beta = \beta_b$ (b) $\beta_k < \beta < \beta_b$ (c) $\beta = \beta_k$ (d) $0 < \beta < \beta_k$

**Figure 3.** The bifurcations of phase portraits of system (1.5) as $\beta$ is varied. Parameter values: $\delta = 0.18, q_c = 0.16, q_h = 0.75, M = 2.15, \sigma = 0.12; \beta_b = 0.1814691367, \beta_k = 0.17199909$

periodic orbit near the straight line $\phi = \phi_m$, respectively. Because the $\phi-$coordinate is almost constant in the segment $\phi_+\phi_-$, $d\phi \approx 0$, so that the third integral in the right hand of (2.1) is $O(\epsilon)$.

By the above discussion, we have the following conclusion:

**Proposition 2.1.** *In the left or right strip neighborhood of a straight line $\phi = \phi_m$, if there exists a family of segments of the periodic orbits of a traveling system, which is very close to the straight line $\phi = \phi_m$, then this family of periodic orbits give rise to a periodic peakon family. As a limit orbit of the periodic peakon family, the homoclinic orbit to an equilibrium point gives rise to a pseudo-peakon solution.*

By using the above result, we have the following theorem:

**Theorem 2.1.** *There exists a parameter group $(\beta, \delta, \sigma, q_c, q_h)$ of system* (1.5)*, such that when the parameter $M$ is varied, system* (1.5) *has the bifurcations of phase portraits shown in Fig.2 (a)-(l). Thus, system* (1.1) *has smooth solitary wave solutions, periodic wave solutions, periodic peakons, pseudo-peakons, compacton families, as well as kink and anti-kink wave solutions.*

For example, considering the orbits in Fig.2 (g), we have

(i) Corresponding to the two homoclinic orbits of system (1.5) defined by $H_1(\phi, y) = 0$, there exist a smooth solitary wave solution (see Fig.4 (b)) and a pseudo-peakon solution (see Fig.4 (a)) of system (1.1).

(ii) Corresponding to the homoclinic orbit of system (1.5) defined by $H_1(\phi, y) = h_1$, there exists a pseudo-peakon solution (see Fig.4 (c)) of system (1.1).

(iii) Corresponding to the family of periodic orbits of system (1.5) defined by $H_1(\phi, y) = h, h \in (0, h_1)$, there exists a family of periodic peakon solutions (see Fig.4 (d)) of system (1.1).

(iv) Corresponding to the family of periodic orbits of system (1.5) defined by $H_1(\phi, y) = h, h \in (h_2, 0)$, there exists a family of smooth periodic solutions (see Fig.4 (f)) of system (1.1).

(v) Corresponding to the family of periodic orbits of system (1.5) defined by $H_1(\phi, y) = h, h \in (0, h_3)$, there exists a family of periodic peakon solutions (see Fig.4 (e)) of system (1.1).

We know from Fig.3 that when $\beta$ is varied, the following conclusion holds:

**Theorem 2.2.** *There exists a parameter group $(M, \delta, \sigma, q_c, q_h)$ of system* (1.5)*, such that when the parameter $\beta$ is varied, system* (1.1) *has smooth solitary wave solutions, periodic wave solutions, compacton families, as well as kink and anti-kink*

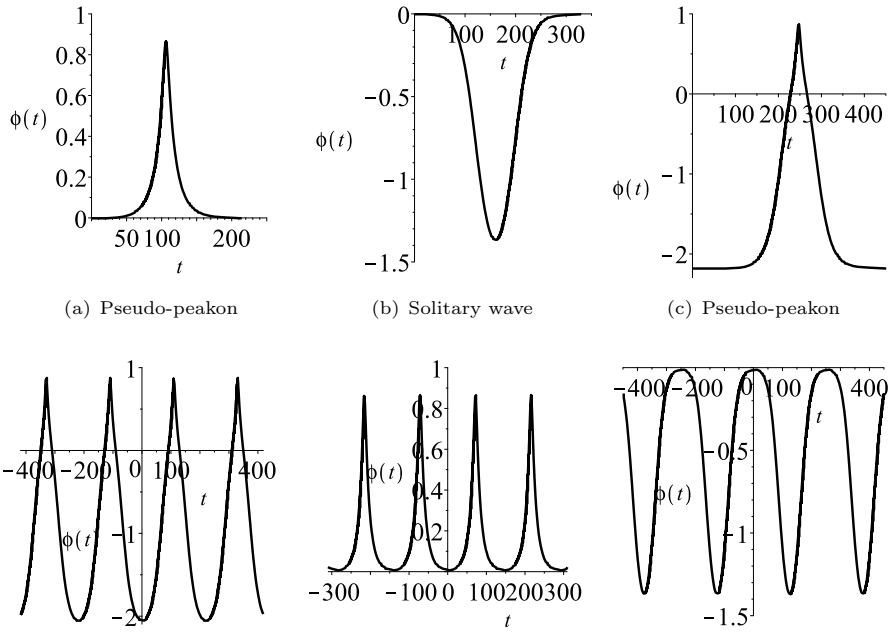


(a) Pseudo-peakon (b) Solitary wave (c) Pseudo-peakon

(d) Periodic peakon (e) Periodic peakon (f) Smooth periodic wave

**Figure 4.** The wave profiles of system (1.5) corresponding to the orbits in Fig.2 (g)

*wave solutions.*

## 3. Bifurcations of phase portraits and dynamical behaviors of solutions of traveling wave system (1.13)

Now, We consider possible bifurcations of phase portraits of system (1.13). To investigate the equilibrium points $E_j(\phi_j, 0)$ of system (1.13), we need to discuss the zeros $\phi_j$ of the function $Q_2(\phi)$. Clearly, $Q_2(0) = 0$, thus the origin $O(0, 0)$ is an equilibrium point of system (1.13). Because $Q_2(\phi)$ depends on the six-parameter group $(\alpha, \beta_1, \beta_2, K_1, K_2, M)$, so it is very difficult to find other equilibrium points of system (1.13) depending on the changes of parameters. We assume that the parameters $\gamma_1$ and $\gamma_2$ are rational numbers such that the exponents $\beta_1 > 1$ and $\beta_2 > 1$. Function $Q_2(\phi)$ is defined in the interval $(-\beta_2 K_2, \phi_d)$, where $\phi_d = \min\left(\beta_1 K_1, \frac{1}{2}M^2\right), K_1 > 0, K_2 > 0$. For a given parameter group, we can use numerical method to find all zeros of $Q_2(\phi)$ in $(-\beta_2 K_2, \phi_d)$.

Let $M(\phi_j, 0)$ be the coefficient matrix of the linearized system of system (1.13) at an equilibrium point $E_j(\phi_j, 0)$ and $J(\phi_j, 0) = \det M(\phi_j, 0)$. We have $J(\phi_j, 0) = -Q_2'(\phi_j)$. Especially,

$$J(0,0) = \frac{1}{M^2} - \frac{\alpha}{K_1}\left(1 - \frac{1}{\beta_1}\right) - \frac{1+\alpha}{K_2}\left(1 - \frac{1}{\beta_2}\right).$$

When $M = \frac{1}{\sqrt{\frac{\alpha}{K_1}\left(1-\frac{1}{\beta_1}\right)+\frac{1+\alpha}{K_2}\left(1-\frac{1}{\beta_2}\right)}} \equiv M_b$, the origin $O(0,0)$ is a cusp. When $M > M_b$ ($M < M_b$), the origin is a saddle point (a center).

Write that $h_0 = H_2(0,0) = 0, h_1 = H_2(\phi_1, 0)$ where $(\phi_1, 0)$ is an equilibrium point of system (1.13) with $-\beta_2 K_2 < \phi_1 < \phi_d$.

For a fixed parameter group $(\alpha, \beta_1, \beta_2, K_1, K_2) = (1.1, \frac{5}{2}, 4, 2, 3)$, by varying the parameter $M$, we have the following bifurcations of the phase portraits of system (1.13):

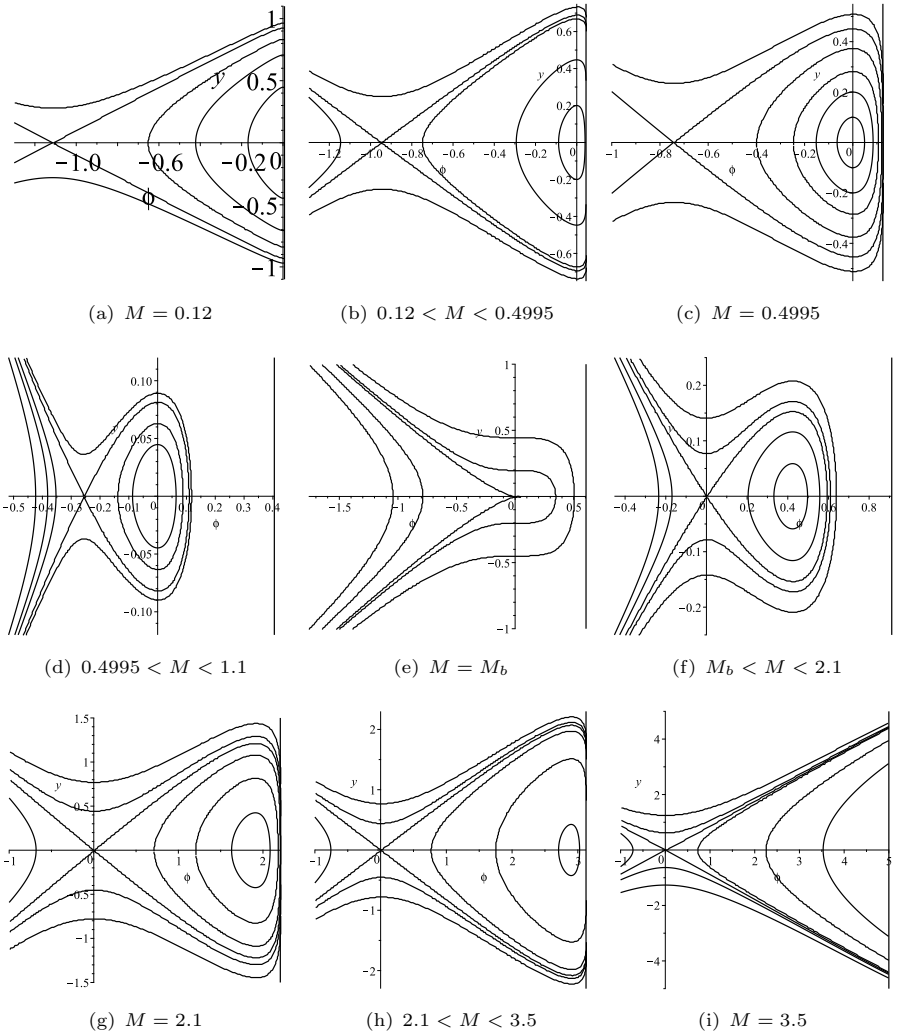

(a) $M = 0.12$ (b) $0.12 < M < 0.4995$ (c) $M = 0.4995$

(d) $0.4995 < M < 1.1$ (e) $M = M_b$ (f) $M_b < M < 2.1$

(g) $M = 2.1$ (h) $2.1 < M < 3.5$ (i) $M = 3.5$

**Figure 5.** The bifurcations of phase portraits of system (1.13) as $M$ is varied. Parameter values: $\alpha = 1.1, \gamma_i = 5/3, \gamma_e = 4/3, K_1 = 2, K_2 = 3; \beta_1 = \frac{5}{2}, \beta_2 = 4; M_b = 1.081476141$

By the above discussion, we have the following conclusion for system (1.13):

**Theorem 3.1.** *There exists a parameter group* $(\alpha, \beta_1, \beta_2 K_1, K_2)$ *of system* (1.13), *such that when the parameter* $M$ *is varied, system* (1.13) *has the bifurcations of*

*phase portraits shown in Fig.5 (a)-(i). Thus, system* (1.8) *has smooth solitary wave solutions, periodic wave solutions, periodic peakons, pseudo-peakons and compacton families.*

For example, considering the orbits in Fig.5, we have

(i) Corresponding to the two homoclinic orbits of system (1.13) defined by $H_2(\phi, y) = h_1$ and $H_2(\phi, y) = 0$ in Fig.5 (d) and Fig.5 (f), respectively, there exist two smooth solitary wave solutions of system (1.8) (see Fig.6 (a)).

(ii) Corresponding to the two families of periodic orbits of system (1.13) defined by $H_2(\phi, y) = h, h \in (h_2, 0)$ in Fig.5 (d) and Fig.5 (f), there exist two families of smooth periodic solutions of system (1.8) (see Fig.6 (b)).

(iii) Corresponding to the two homoclinic orbits of system (1.13) defined by $H_2(\phi, y) = h_1$ and $H_2(\phi, y) = 0$ in Fig.5 (c) and Fig.5 (g), respectively, there exists a pseudo-peakon solution of system (1.8) (see Fig.6 (c)).

(iv) Corresponding to the two families of periodic orbits of system (1.13) defined by $H_2(\phi, y) = h, h \in (0, h_1)$ in Fig.5 (c) and Fig.5 (g), there exist two families of periodic peakon solutions of system (1.8)(see Fig.6 (d)).

(v) Corresponding to the family of orbits of system (1.5) defined by $H_2(\phi, y) = h, h \in (0, h_3)$, intersecting transversely the straight line $\phi = \phi_d$, there exists a family of compacton solutions of system (1.8) (see Fig.6 (e)).

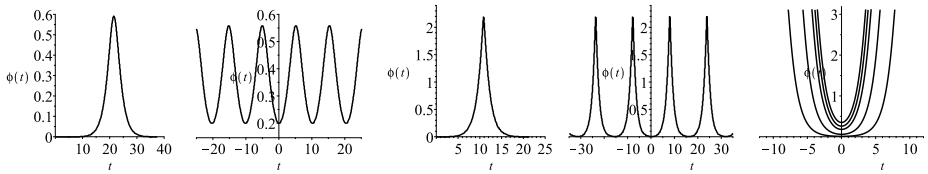


**Figure 6.** The different wave profiles of system (1.13)

# 4. Bifurcations of phase portraits and dynamical behaviors of solutions of traveling wave system (1.21)

In this section, we consider possible bifurcations of phase portraits of system (1.21). To investigate the equilibrium points $E_j(\psi_j, 0)$ of system (1.21), we need to discuss the zeros $\psi_j$ of the function $Q_3(\psi)$. Clearly, $Q_3(0) = 0$, thus the origin $O(0, 0)$ is an equilibrium point of system (1.21). The function $Q_3(\psi)$ depending on five-parameter group $(\alpha_p, \gamma, v_0, p, M)$ is very complicated. It is very difficult to find all equilibrium points of system (1.21) depending on the changes of parameters. We notice that when $0 < p < 1$ and $\alpha_p > 0$, function $n_i(\psi)$ has an unique negative zero $\psi = \psi_{mul}$. Therefore, the function $Q_3(\psi)$ has a multiple zero $\psi = \psi_{mul}$, i.e., $E_m(\psi_{mul}, 0)$ is a high-order equilibrium point of system (1.21). For a given parameter group, we can use numerical method to find the zeros of $Q_3(\psi)$ in $\psi-$axis.

Let $M(\psi_j, 0)$ be the coefficient matrix of the linearized system of system (1.21) at an equilibrium point $E_j(\psi_j, 0)$ and $J(\psi_j, 0) = \det M(\psi_j, 0)$. We have $J(\psi_j, 0) =$

$-Q_3'(\psi_j) = S_3''(\psi_j)$. Specially,

$$J(0,0) = S_3''(0) = \frac{M^2(M_d^2 - M_0^2)}{M_d^2(M_d^2 - M_1^2)}, \quad M_1^2 = \frac{p}{1+\alpha_p(1-p)}, \; M_0^2 = \gamma^2 M_1^2.$$

It implies that when $M_0 < M_d < M_1$, i.e.,

$$M_{cusp} \equiv \gamma\left(v_0 + \sqrt{\frac{p}{1+\alpha_p(1-p)}}\right) < M < \left(\gamma v_0 + \sqrt{\frac{p}{1+\alpha_p(1-p)}}\right) \equiv M_{inf},$$

$J(0,0) < 0$, the origin $O(0,0)$ is a saddle point. When $M_d = M_0$, i.e., $M = M_{cusp}, J(0,0) = 0$, the origin $O(0,0)$ is a cusp. When $M_d = M_1$, i.e., $M = M_{inf}$, for the function $D(\psi) = n_i^3(\psi) - p^2 M_d^2 n_i'(\psi)$, we have $D(0) = 0$, i.e., $\psi_s = 0$ and $\lim_{\psi\to 0} Q_3(\psi) = -\infty$. We do not consider this case.

Write that $h_j = H_3(\psi_j, 0)$, where $(\psi_j, 0)$ is an equilibrium point of system (1.21). Especially, we see from (1.22) and (1.23) that $h_0 = H_3(0,0) = H_3(\psi_{mul}, 0) = 0 = h_{mul}$.

For the fixed parameter group $(\alpha_p, \gamma, p, v_0) = (0.1, 0.7071, 0.75, 0.2)$ given by [13], by varying the parameter $M$, we have the following graphs of function $Q_3(\psi)$:

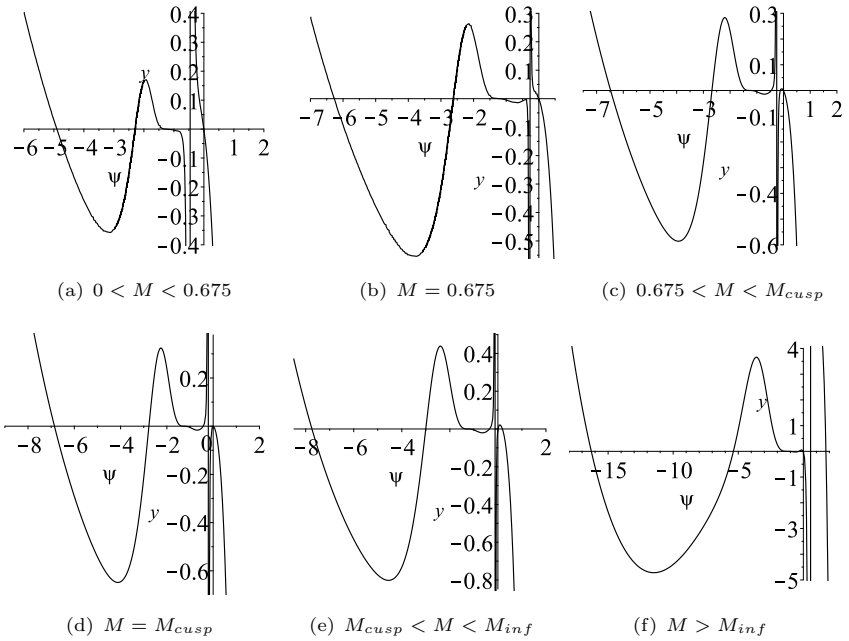


(a) $0 < M < 0.675$ (b) $M = 0.675$ (c) $0.675 < M < M_{cusp}$

(d) $M = M_{cusp}$ (e) $M_{cusp} < M < M_{inf}$ (f) $M > M_{inf}$

**Figure 7.** The graphs of function $Q_3(\psi)$ of system (1.21) as $M$ is varied

We know that

(1) When $0 < M < 0.675$, system (1.21) has four equilibrium points $E_1(\psi_1, 0)$, $E_2(\psi_2, 0), E_3(\psi_{mul}, 0)$ and $O(0,0)$ with $\psi_1 < \psi_2 < \psi_{mul} < \psi_s < 0 < \psi_4$.

(2) When $0.675 < M < M_{cusp}$, system (1.21) have six equilibrium points $E_1(\psi_1, 0), E_2(\psi_2, 0), E_3(\psi_{mul}, 0), E_4(\psi_4, 0), E_5(\psi_5, 0)$ and $O(0,0)$ with $\psi_1 < \psi_2 < \psi_{mul} < \psi_4 < \psi_s < \psi_5 < 0$.

(3) When $M_{cusp} < M < M_{inf}$, system (1.21) have six equilibrium points $E_1(\psi_1, 0), E_2(\psi_2, 0), E_3(\psi_{mul}, 0), E_4(\psi_4, 0), O(0, 0)$ and $E_5(\psi_5, 0)$ with $\psi_1 < \psi_2 < \psi_{mul} < \psi_4 < \psi_s < 0 < \psi_5$.

(4) When $M > M_{inf}$, system (1.21) have six equilibrium points $E_1(\psi_1, 0)$, $E_2(\psi_2, 0)$, $E_3(\psi_{mul}, 0)$, $E_4(\psi_4, 0), O(0, 0)$ and $E_5(\psi_5, 0)$ with $\psi_1 < \psi_2 < \psi_{mul} < \psi_4 < 0 < \psi_s < \psi_5$.

Under the above parameter condition, by varying the parameter $M$, we have the following bifurcations of phase portraits of traveling wave system (1.21)(the figures $(a_1) - (f_1)$ in Fig.8 are large figures, the figures $(a_2) - (f_2)$ are the figures near the singular line $\psi = \psi_s$ and the origin $O(0, 0)$):

To sum up, from the above discussion, we have the following conclusion:

**Theorem 4.1.** *Assume that* $0 < p < 1$. *There exists a parameter group* $(\alpha_p, \gamma, v_0, p)$ *of system* (1.21), *such that when the parameter* $M$ *is varied, system* (1.21) *has the bifurcations of phase portraits shown in Fig.8 (a)-(f). Therefore, these phase orbits can give rise to smooth solitary wave solutions, periodic wave solutions, periodic peakons, pseudo-peakons and compacton families of system* (1.14).

Specially, for any $M \in (0, \infty), M \neq M_{inf}$, corresponding to the homoclinic orbit defined by $H_3(\psi, y) = h_1$, there exists a smooth solitary wave solution with lager amplitude. Corresponding the the periodic orbit family defined by $H_3(\psi, y) = h, h \in (h_2, h_1)$, enclosing the equilibrium point $E_1(\psi_1, 0)$, there exists a family of smooth periodic wave solutions of system (1.14).

For two examples, we consider two phase portraits Fig.8 (a) and Fig.8 (f), and have the following two conclusions:

**Theorem 4.2.** *Assume that* $0 < p < 1$. *In this case, system* (1.21) *has the phase portrait Fig.8 (a) and* $h_1 < h_0 = 0 = h_{mul} < h_2 < \infty$, *then we have*

*(1) Corresponding to the family of periodic orbits defined by* $H_3(\psi, y) = h, h \in (h_1, h_2)$, *enclosing the equilibrium point* $E_1(\psi_1, 0)$, *system* (1.14) *has a family of smooth periodic wave solutions (see Fig.9 (a)).*

*(2) Corresponding to the two homoclinic orbits to equilibrium point* $E_2(\psi_2, 0)$ *defined by* $H_3(\psi, y) = h_2$, *enclosing the equilibrium points* $E_1(\psi_1, 0)$ *and* $E_{mul}(\psi_{mul}, 0)$, *respectively, system* (1.14) *has a smooth solitay wave solution (see Fig.9 (b)) and a pseudo-peakon solution (see Fig.9 (c)).*

*(3) Corresponding to the periodic orbit family defined by* $H_3(\psi, y) = h, h \in (h_{mul}, h_2)$, *enclosing equilibrium point* $E_{mul}(\psi_{mul}, 0)$, *system* (1.14) *has a family of periodic peakon solutions (see Fig.9 (e)).*

*(4) Corresponding to the family of periodic orbits defined by* $H_3(\psi, y) = h, h \in (h_2, h_{m1})$, *enclosing three equilibrium points* $E_1(\psi_1, 0), E_2(\psi_2, 0)$ *and* $E_{mul}(\psi_{mul}, 0)$, *system* (1.14) *has a family of large periodic peakon solutions (see Fig.9 (f)), where* $h_{m1} > h_2$ *is a large number.*

*(5) Corresponding to the family of periodic orbits defined by* $H_3(\psi, y) = h, h \in (0, h_{m2})$, *enclosing the equilibrium point* $O(0, 0)$, *system* (1.14) *has a family of periodic peakon solutions (see Fig.9 (g)), where* $h_{m2} > 0$ *is a large number.*

*(6) Corresponding to the two families of open orbits defined by* $H_3(\psi, y) = h, h \in (h_{m1}, \infty)$ *and* $h \in (h_{m2}, \infty)$, *respectively, transversely intersecting the singular straight line* $\psi = \psi_s$, *system* (1.14) *has two families of compacton solutions (see Fig.9 (d), (h)).*

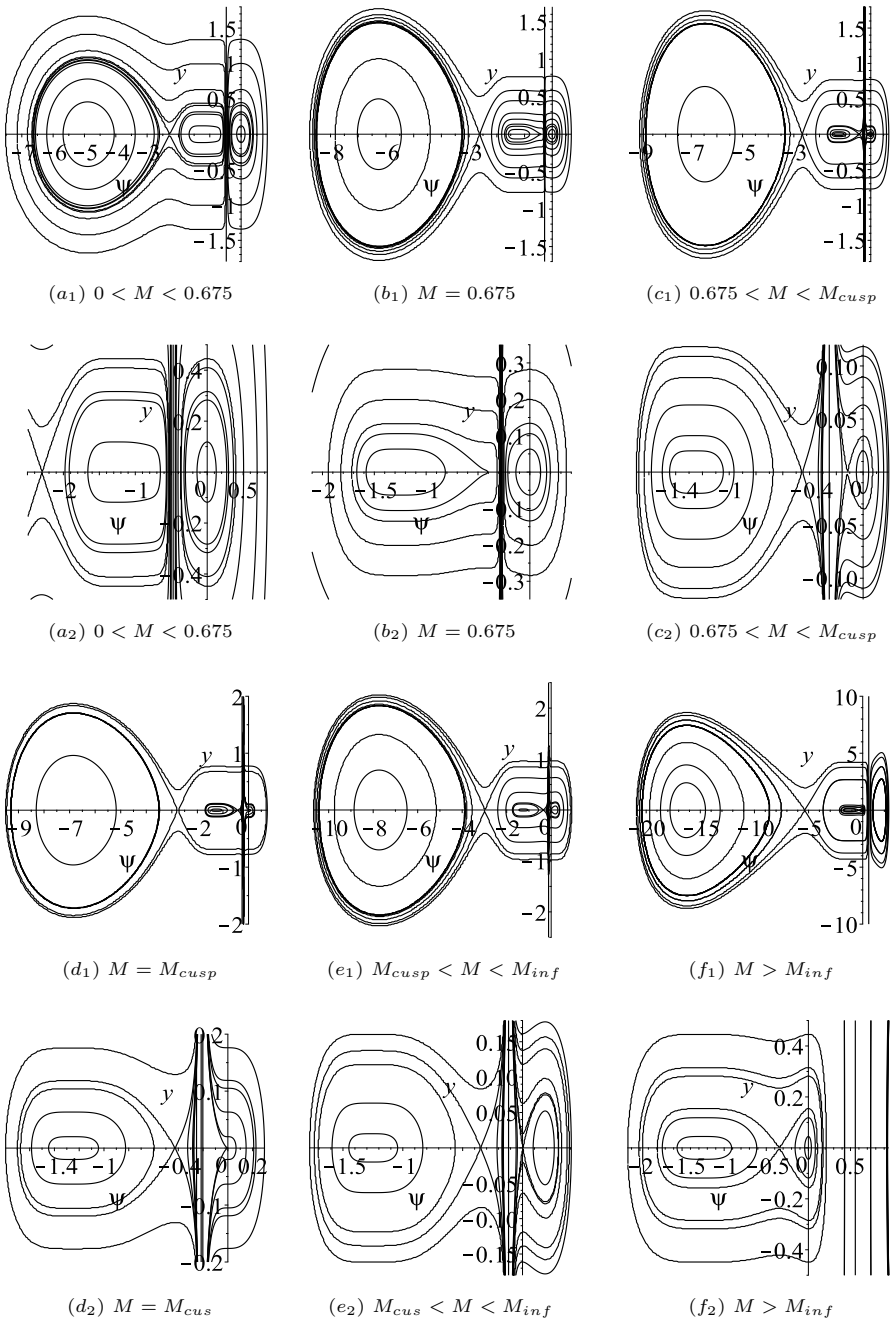


($a_1$) $0 < M < 0.675$ ($b_1$) $M = 0.675$ ($c_1$) $0.675 < M < M_{cusp}$

($a_2$) $0 < M < 0.675$ ($b_2$) $M = 0.675$ ($c_2$) $0.675 < M < M_{cusp}$

($d_1$) $M = M_{cusp}$ ($e_1$) $M_{cusp} < M < M_{inf}$ ($f_1$) $M > M_{inf}$

($d_2$) $M = M_{cus}$ ($e_2$) $M_{cus} < M < M_{inf}$ ($f_2$) $M > M_{inf}$

**Figure 8.** The bifurcations of phase portraits of system (1.21) as $M$ is varied. Parameter values: $\alpha_p = 0.1$, $\gamma = \cos\frac{\pi}{4}$, $p = 0.75$, $v_0 = 0.2$. In this case, $M_{cusp} = 0.7462797351$, $M_{inf} = 0.9968202790$.

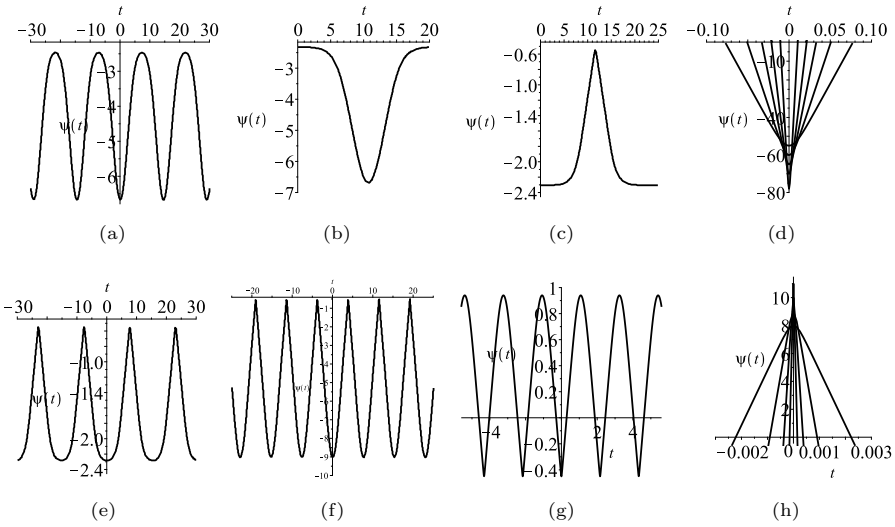


**Figure 9.** The wave profiles of system (1.14) corresponding to the orbits in Fig.8 (a)

**Theorem 4.3.** *Assume that* $0 < p < 1$ *and system* (1.21) *has the phase portrait Fig.8 (f). In this case, there exists six equilibrium points. We have* $h_1 < h_0 = 0 = h_{mul} < h_4 < h_5 < h_2 < \infty$. *Then,*

*(1) Corresponding to the periodic orbit family defined by* $H_3(\psi, y) = h, h \in (h_1, h_2)$, *enclosing the equilibrium point* $E_1(\psi_1, 0)$, *system* (1.14) *has a family of smooth periodic wave solutions (see Fig.10 (a)).*

*(2) Corresponding to the two lager homoclinic orbit loops to the equilibrium point* $(E_2(\psi_2, 0)$ *defined by* $H_3(\psi, y) = h_2$, *enclosing the equilibrium points* $(E_1(\psi_1, 0)$ *and three equilibrium points* $E_{mul}(\psi_{mul}, 0), E_4(\psi_4, 0), O(0, 0)$, *respectively, system* (1.14) *has a smooth solitay wave solution (see Fig.10 (b)) and a pseudo-peakon solution (see Fig.10 (c)).*

*(3) Corresponding to the periodic orbit family defined by* $H_3(\psi, y) = h, h \in (h_2, h_{m1})$, *enclosing five equilibrium points* $E_1(\psi_1, 0), E_2(\psi_2, 0), E_{mul}(\psi_{mul}, 0), O(0, 0)$ *and* $E_4(\psi_4, 0)$, *system* (1.14) *has a family of large periodic peakon solutions (see Fig.10 (d)), where* $h_{m1} > h_2$ *is a large number.*

*(4) Corresponding to the two homoclinic orbits to the equilibrium point* $(E_4(\psi_4, 0)$ *defined by* $H_3(\psi, y) = h_4$,, *enclosing the equilibrium points* $E_{mul}(\psi_{mul}, 0)$ *and the origin* $O(0, 0)$, *respectively, system* (1.14) *has a smooth solitary wave solution (see Fig.10 (f)) and a pseudo-peakon solutions (see Fig.10 (g)).*

*(5) Corresponding to the periodic orbit family defined by* $H_3(\psi, y) = h, h \in (h_4, h_2)$, *enclosing three equilibrium points* $E_{mul}(\psi_{mul}, 0), E_4(\psi_4, 0)$ *and* $O(0, 0)$, *system* (1.14) *has a family of periodic peakon solutions (see Fig.10 (e)), where* $h_{m1} > h_2$ *is a large number.*

*(6) Corresponding to the periodic orbit family defined by* $H_3(\psi, y) = h, h \in (h_5, h_{m2})$, *enclosing the equilibrium point* $O(0, 0)$, *system* (1.14) *has a family of periodic peakon solutions (see Fig.10 (h)), where* $h_{m2} > 0$ *is a large number.*

*(7) Corresponding to two open orbit families defined by* $H_3(\psi, y) = h, h \in (h_{m1}, \infty)$ *and* $h \in (h_{m2}, \infty)$, *respectively, transversely intersecting the singular straight line* $\psi = \psi_s$, *system* (1.14) *has two families of compacton solutions.*

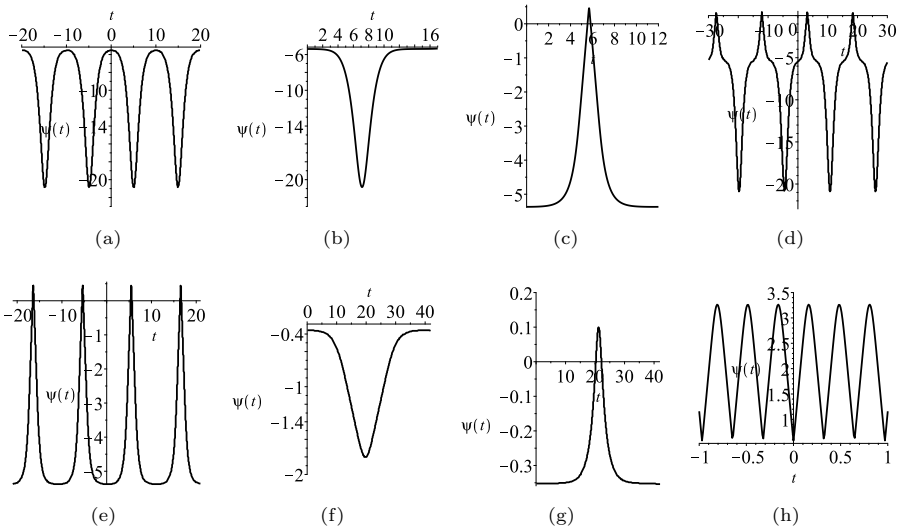


**Figure 10.** The wave profiles of system (1.14) corresponding to the orbits in Fig.8 (f)

Similarly, considering other phase portraits in Fig.8, we can give corresponding results about the existence of various traveling wave solutions.

## Acknowledgments

We are very grateful to our esteemed Mentor, Professor Jibin Li in the School of Mathematical Sciences, Huaqiao University, for his valuable instructions and suggestions on our paper.

## References

[1] G. C. Das, *Rotation as a progenitor of various solitary waves in magnetized plasmas,* Chaos Solit. Fract., 2017, 101, 33–40.

[2] S. Ghebache, M. Tribeche, *Nonlinear ion-acoustic double-layers in electronegative plasmas with electrons featuring Tsallis distribution,* Physica A, 2016, 447, 180–187.

[3] S. Ghebache, M. Tribeche, *Arbitrary amplitude ion-acoustic solitary waves in electronegative plasmas with electrons featuring Tsallis distribution,* Physica A, 2017, 483, 193–200.

[4] W. F. El Taibany, M. Tribeche, *Nonlinear ion-acoustic solitary waves in electronegative plasmas with electrons featuring Tsallis distribution,* Phys. Plasmas, 2012, 19, 024507.

[5] M. M. Hatami, M. Tribeche, *Arbitrary amplitude ion-acoustic solitary waves in a two-temperature nonextensive electron plasma,* Physica A, 2018, 491, 55–63.

[6] J. Li, G. Chen, *Bifurcations of travelling wave solutions for four classes of nonlinear wave equations,* 2005, 15(12), 3973–3998.

[7] J. Li, G. Chen, *On a class of singular nonlinear traveling wave equations,* Int. J. Bifurcation and Chaos, 2007, 17, 4049–4065.

[8] J. Li, *Singular Nonlinear Traveling Wave Equations: Bifurcations and Exact Solutions,* Science Press, Beijing, 2013.

[9] J. Li, W. Zhou, G. Chen, *Understanding peakons, periodic peakons and compactons via a shallow water wave equation,* Int. J. Bifurcation and Chaos, 2016, 26(12), 1650207.

[10] J. Li, *Periodic peakons, pseudo-peakons and compactons of ion-acoustic wave model in electronegative plasmas with electrons featuring tsallis distribution,* Int. J. of Bifurcation and Chaos, 2018, 28(1), 1850015.

[11] J. Li, *Solitary waves, periodic peakons and pseudo-peakons of the nonlinear acoustic wave model in rotating magnetized plasma,* Int. J. of Bifurcation and Chaos, 2018, 28(4), 1850054.

[12] J. Li, *Geometric properties and exact travelling wave solutions for the generalized Burger-Fisher equation and the Sharma-Tasso-Olver equation,* J. of Nonlinear Modeling and Analysis, 2019, 1(1), 1–10.

[13] O. R. Rufai, R. Bharuthram, *Obliquely propagating low-frequency magnetospheric electrostatic solitary waves in the presence of an oxygen-ion beam,* Commun Nonlinear Sci. Numer. Simulat., 2019, 68, 160–168.

[14] S. Sultana1, R. Schlickeiser, *Fully nonlinear heavy ion-acoustic solitary waves in astrophysical degenerate relativistic quantum plasmas,* Astrophys Space Sci., 2018, 363, 103.

[15] R. Z. Sagdeev, *Reviews of Plasma Physics,* in: M.A. Leontovich (Ed.), Consultants Bureau, New York, 1966.